Bull. Sch. Health. Sci., Kagoshima Univ.
13(2) : 9 - 14, 2003

Visualization of 3D Human Motion Captured with an Optical Motion Analysis System

Kiyohiro Fukudome, Ryouji Kiyama, and Norio Morimoto

ABSTRACT: To visualize dynamic 3-dimensional (3D) human motion data captured with optical motion analysis systems, a Windows program that reads motion data in a comma-separated-values (CSV) format file, transforms the 3D coordinates datasets to joint angles, and writes the joint angle data as a BVH format file used in 3D applications such as Poser, has been developed. The Windows program was examined by using a test CSV format file that contains 3D motion data of human treadmill walking (300 frames). The treadmill walking was subsequently examined to be replicated from a generated BVH format file into a virtual 3D space of computer after an animation tool Poser imported its file. It was confirmed that the Window program itself works satisfactorily though abnormal rotations result in the Poser's automatic correction were seen in the virtual treadmill walking.

Key words: human motion, motion capture, treadmill walking, BVH format, Poser, Windows program

Introduction

Motion capture has been used extensively for creating 3D animations and understanding human motions. Recent progress in cpu enables us to create or display dynamic human motion. The Visible Human Project plans to create the normal male and female human bodies in virtual 3D space[1, 2]. It has generated over 18000 digitized sections of the human bodies to date, though their sections are static. A Java applet program has been developed to animate a web-based interactive human model whose motions use motion-captured data[3]. Computer simulation of human motion would become progressively more physically realistic and more natural-looking.

When clinical gait data are captured with motion analysis systems, the motion and forces of the patient's leg joints are important but some of his/her body features such as skin and hair color, facial characteristics would become negligible. If a program can produce the dynamic virtual figure without the patient's features, it would be utilized not only to improve protection of patient privacy but also to share information easily about patients via the World Wide Web. Moreover, while postural responses to unexpected perturbations were studied[4, 5], virtual robots, if developed, would be used to analyze the response of a human body to unexpected external perturbations.

In the present study, a Windows program has been developed to transform experimentally obtained 3D-coordinates datasets to joint angles, and to write the data as a BVH format file that can be imported by 3D applications such as Poser. Using treadmill walking data that are captured with a motion analysis system, we examined the program and its generated BVH file. Some problems will be described in this paper. The present study would, however, open up the possibility to simulate human motion of privacy-protected patients in a virtual environment.

Course of Physical Therapy, School of Health Sciences, Faculty of Medicine, Kagoshima University, 8-35-1 Sakuragaoka, Kagoshima 890-8520, Japan.
E-mail: fukudome@health.nop.kagoshima-u.ac.jp
Tel: 099-275-6741

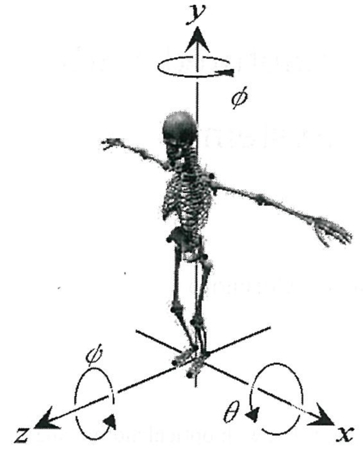

Figure 1. Base human model in the global frame of reference. Markers placed on individual joints are shown as dots in the Figure. The direction of rotation follows the right hand rule, as indicated as rings around axes.

Methods

A. Motion measurement and base human model

An unimpaired, male participant aged 21 years walked with a velocity of 5.6 km/h for 5 seconds on a motorized treadmill, carrying a set of 10 markers placed on his active joints: shoulders, thighs, knees, ankles, and toes. During the treadmill walking, dynamic 3D human motion data were captured with an optical motion analysis system Anima Locus MA5250A at a sampling rate of 60 frames per second. A series of data was saved as a CSV (comma separated values) format file. It should be noted that the obtained data provide maker coordinates in a laboratory frame of referenece.

Human motion involves the various body segments in motion. Then the total body motion is the result of the combined movements of the individual body segments. However the individual segmental movements are dependent on each other because of the hierarchical linkage of the segments. A rough base human model with 10 segment was used in the present study. These 10 segments are connected by triaxis hinge joints as shown in Figure 1.

B. Developmental environment

A development environment, National Instruments LabWindows/CVI 5.0, was used to write a program that will run under Microsoft Windows, with graphical user interfaces. Its source files were written and compiled in C language. A personal computer has dual Pentium IV (1 MHz) and ca. 1.6 GB of the system memory was used for the program development.

```
ROOT Hip
{
        OFFSET 0.00   0.00   0.00
        CHANNELS 6 Xposition Yposition Zposition Xrotation Zrotation Yrotation
        JOINT Abdomen
        {
                OFFSET 0.000000 0.000000 0.000000
                CHANNELS 3 Xrotation Zrotation Yrotation
                JOINT Chest
                {
                        OFFSET 0.000000 5.018152 -1.882228
                        CHANNELS 3 Xrotation Zrotation Yrotation
                        JOINT Neck
                        {
                        ...
                        }
                        JOINT Left Collar
                        {
                                OFFSET 0.599237 8.316447 0.784897
                                CHANNELS 3 Xrotation Zrotation Yrotation
                                JOINT Left Shoulder
                                {
                                ...
                                }
                        }
                        JOINT Right Collar
                        {
                                OFFSET -0.599237 8.316447 0.784897
                                CHANNELS 3 Xrotation Zrotation Yrotation
                                JOINT Right Shoulder
                                {
                                ...
                                }
                        }
                }
        }
        JOINT Left Thigh
        {
                OFFSET 4.500466 -6.400484 -1.832696
                CHANNELS 3 Xrotation Zrotation Yrotation
                JOINT Left Shin
                {
                ...
                }
        }
        JOINT Right Thigh
        {
                OFFSET -4.500466 -6.400484 -1.832696
                CHANNELS 3 Xrotation Zrotation Yrotation
                JOINT Right Shin
                {
                ...
                }
        }
}
```

Figure 2. Example of the hierarchy section in a BVH format file. The details are described in the text.

C. BVH format

The BVH (Bio Vision Hierarchical) file format defined by BioVision has extensively been used to describe captured-motion[6]. We chose this file format because many commercial software programs have supported its file format. Its text-based file consists of two parts, the hierarchy and motion-data sections as described in detail below.

D. Hierarchy section of BVH file

The hierarchy defines the tree structure of segments. Figure 2 shows an example of the hierarchy section. Each hierarchical segment is described in this section with the x, y, and z offset values from its parent, the rotation angles around the segment's local x-, y-, and z-axes, and its child segment(s). A parent segment can have more than one child but the child can only have one parent. The motion of the child segment also depends on the motion of the upper

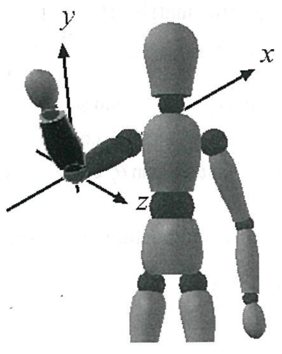

Figure 3. Child-parent relationship. The endpoint of the child segment of right forearm is defined in a local frame of reference set to its parent of right shoulder.

segments including its parent segment, because the rotations of the child segment are defined in its parent frame.

The order of rotation is important and described in detail later in the next section. Figure 3 shows a child segment (right forearm) in a local frame of reference which is defined by its parent (of right forearm). Then the local frame of reference does not usually corresponds to the global frame of reference. It should therefore be noted that the coordinates of almost all of the segments are described in the different frame of reference. Only a root segment involves absolute position (x, y, z) additionally and then the number of channels becomes 6 (See the Figure).

E. Motion-data section of BVH file

The second section contains the number of frames, the frame rate in seconds per frame, and a series of the numeric frame data as shown in Figure 4. Each entry of the numeric frame data must appear in the same order as the channels

```
MOTION
Frames:300
Frame Time:0.016666
0.12        53.71 -6.64  0.00  1.48  0.62 -0.50  3.44-11.07  0.00
             0.00  0.00  0.00  0.00  0.00  0.00  0.00  0.00  0.00
             0.00  0.00  0.00  0.00  0.00  0.00  0.00  0.00  0.00
             0.00  0.00  0.00  0.00  0.00  0.00  0.00  0.00  0.00
             0.00  0.00  0.00  0.00  0.00-24.16  2.02  0.00  0.32
            -7.13  0.00 17.93  0.00  5.86  7.70  1.84  0.00 18.23
            10.13  0.00 28.94  0.00-19.82
0.17        53.55 -6.61  0.00  1.64  0.93 -0.93  3.41-11.61  0.00
             ...
            10.60  0.00 29.74  0.00-20.93
0.17        53.35 -6.38  0.00  2.17  1.70 -2.35  3.04-11.83  0.00
             ...
            10.27  0.00 31.88  0.00-22.50
...
```

Figure 4. Example of the motion-data section in a BVH format file. The details are described in the text.

defined in the hierarchy section. The angular values are expressed in degrees. Only for the root segment, the 3 translation values should be given.

Although the motion capture procedure determines the point of the individual joints in a common laboratory-frame of reference, the BVH file requires not only the rotation angles in a local frame of reference which is defined in and is rotating with its parent segment, but also the coordinates for the root in the laboratory frame of reference. The desired rotational transforms for the joints should be extracted from the motion capture data at each frame of the motion sequence.

Algorithms

A. Coordinates in global frame of reference

Let the start point of the root line segment be $\mathbf{p}^0_{i1}$ and the endpoint $\mathbf{p}^0_{i2}$ in the base human model where a subscript j denotes a chain of line segments in the hierarchical tree. It should be noted that the first segment's endpoint becomes the start point of the next segment. Starting with the joint nearest the endpoint $\mathbf{p}^0_{i1}$, rotate the joint so that the current endpoint moves to the new endpoint $\mathbf{p}^0_{i2}$ measured by the motion capture. The coordinates transformation is expressed as

$$\mathbf{p}_{i2} = \mathbf{R}_{i1}(\mathbf{p}^0_{i2} - \mathbf{p}^0_{i1}) + \mathbf{p}_{i1}. \tag{1}$$

where the rotation matrix $\mathbf{R}_{i1}$ is a product of three matrices, $\mathbf{R}^x_{ij}, \mathbf{R}^y_{i1}$, and $\mathbf{R}^z_{i1}$, of rotation around x-, y-, and z-axes and the commutative order of rotation should clearly be indicated as the order of the channels of the hierarchy section in the BVH format file. The rotation matrix elements and unknown rotation angles of the root can therefore be calculated from Equation (1).

B. Coordinates of segment in local frame of reference

We assume that a segment length remains unchanged during a motion sequence, i. e., $|\mathbf{L}_{ij}| = |\mathbf{l}_{ij}| = \text{const}$, where $\mathbf{L}_{ij} = \mathbf{p}_{ij+1} - \mathbf{p}_{ij}$ and $\mathbf{l}_{ij} = \mathbf{p}^0_{ij+1} - \mathbf{p}^0_{ij}$, being row vectors. Generally, the endpoint of the j'th segment $\mathbf{p}_{ij+1}$ are given by the equation

$$\mathbf{L}_{ij} = \mathbf{R}_{i1}\mathbf{R}_{i2}\mathbf{R}_{i3}\cdots\mathbf{R}_{ij}\mathbf{l}_{ij} = \left(\prod_{j'=1}^{j}\mathbf{R}_{ij'}\right)\mathbf{l}_{ij} \tag{2}$$

Equation (2) indicates that rotation of the parent affects rotation of lower segments including all its children. Then the rotation angles of the j'th segment are calculated from

$$\mathbf{R}_{ij-1}^{-1}\cdots\mathbf{R}_{i2}^{-1}\mathbf{R}_{i1}^{-1}\mathbf{L}_{ij} = \mathbf{R}_{ij}\mathbf{l}_{ij}. \tag{3}$$

The individual angles of the upper segments should be known a priori when we use the equation to find the rotation angles of the j'th segment. This means that the calculation begins for the most upper segment, i. e., root. It is emphasized that a certain local transformation of the child is concatenated with the local transformation of its parent as shown in Equation (3).

C. Three rotation matrices and their commutative order for describing segment vector

For the root, the rotation matrix $\mathbf{R}_{ij}$ can be written as

$$\mathbf{R}_{ij} = \mathbf{R}^{x}{}_{ij}\mathbf{R}^{z}{}_{ij}\mathbf{R}^{y}{}_{ij} \tag{5}$$

when the order of rotation is $\mathbf{R}^{y}{}_{ij}$ first, then $\mathbf{R}^{z}{}_{ij}$, and $\mathbf{R}^{x}{}_{ij}$. These three different matrices describe their rotation around local x−, y−, and z−axes:

$$\mathbf{R}^{x}{}_{ij} = \begin{pmatrix} 1 & 0 & 0 \\ 0 & \cos\theta_{ij} & -\sin\theta_{ij} \\ 0 & \sin\theta_{ij} & \cos\theta_{ij} \end{pmatrix}, \tag{6}$$

$$\mathbf{R}^{y}{}_{ij} = \begin{pmatrix} \cos\varphi_{ij} & 0 & \sin\varphi_{ij} \\ 0 & 1 & 0 \\ -\sin\varphi_{ij} & 0 & \cos\varphi_{ij} \end{pmatrix}, \tag{7}$$

and

$$\mathbf{R}^{z}{}_{ij} = \begin{pmatrix} \cos\psi_{ij} & -\sin\psi_{ij} & 0 \\ \sin\psi_{ij} & \cos\psi_{ij} & 0 \\ 0 & 0 & 1 \end{pmatrix}. \tag{8}$$

Generally, the segment has its intrinsic order of rotation operation which is not the same as that for the other segments. We can exactly rotate a segment by performing three rotation operations in their intrinsic order specified in the hierarchy section.

Though a 3-dimensinal object, the segment is measured as a line having the start point and endpoint, under the present experimental conditions. The rotation around the long axis of the line segment is not observable. For this reason, the rotation can be realized with the two operators. In the case of a segment with an order of rotation y, z and x mentioned to be "Xrotation Zrotation Yrotation" in a channel line that appears in the hierarchy section, the first operator $\mathbf{R}^{y}{}_{ij}$ becomes meaningless when the position of the segment is transformed to a new position on a standard figure setup to base a biped character:

$$\mathbf{R}_{ij} = \mathbf{R}^{x}{}_{ij}\mathbf{R}^{z}{}_{ij}\mathbf{R}^{y}{}_{ij} = \begin{pmatrix} \cos\psi_{ij} & -\sin\psi_{ij} & 0 \\ \cos\theta_{ij}\sin\psi_{ij} & \cos\theta_{ij}\cos\psi_{ij} & -\sin\theta_{ij} \\ \sin\theta_{ij}\sin\psi_{ij} & \sin\theta_{ij}\cos\psi_{ij} & \cos\theta_{ij} \end{pmatrix} \tag{9}$$

where we change the matrix $\mathbf{R}^{y}{}_{ij}$ to a 3 × 3 unit matrix. Substituting Equation (9) into the Equation (3), we get

$$\begin{pmatrix} L_{ij}^{x} \\ L_{ij}^{y} \\ L_{ij}^{z} \end{pmatrix} = \begin{pmatrix} \cos\psi_{ij} & -\sin\psi_{ij} & 0 \\ \cos\theta_{ij}\sin\psi_{ij} & \cos\theta_{ij}\cos\psi_{ij} & -\sin\theta_{ij} \\ \sin\theta_{ij}\sin\psi_{ij} & \sin\theta_{ij}\cos\psi_{ij} & \cos\theta \end{pmatrix} \begin{pmatrix} 0 \\ l_{ij}^{y} \\ 0 \end{pmatrix}.$$

Finally, we obtain two important equations:

$$\sin\psi_{ij} = -(L_{ij}^{x} / l_{ij}^{y}) \tag{10}$$

and

$$\tan\theta_{ij} = (L_{ij}^{z} / L_{ij}^{y}) \tag{11}$$

that are used to calculate the rotation angles, ψ_{ij} and θ_{ij} expressed in the local frame of reference when the physically measurable quantity $\mathbf{L}_{ij}$ is given in the global frame of reference. Similarly, for $\mathbf{R}_{ij} = \mathbf{R}^{z}{}_{ij}\mathbf{R}^{y}{}_{ij}\mathbf{R}^{x}{}_{ij}$ in the order of rotation around x−, y−, and z−axes, we obtain equations, $\sin\theta_{ij} = -(L_{ij}^{z}/l_{ij}^{x})$ and $\tan\phi_{ij} = (L_{ij}^{y}/l_{ij}^{x})$. For $\mathbf{R}_{ij} = \mathbf{R}^{y}{}_{ij}\mathbf{R}^{x}{}_{ij}\mathbf{R}^{z}{}_{ij}$ in the order of rotation around z−, x−, and y−axes, $\sin\theta_{ij} = -(L_{ij}^{y}/l_{ij}^{z})$ and $\tan\phi_{ij} = (L_{ij}^{x}/l_{ij}^{z})$ The developed program chooses a pair of equations from these equations including Equations (10) and (11), and uses them for determining the rotation angles of the segment, considering the order of its rotation.

D. Calculation of coordinates of point for imperfect root segment

There is not a direct measure of the position of the root segment hip in the present study. Such a case would occur quite frequently when we lack sensors or high-performance-computer necessary for motion capture. Therefore we need to estimate the values for the unknown and important position of the root segment. The participant holds the same relative locations of the rotation centers (start points) for the hip and right and left thighs as the standard figure. Then we set

$$\mathrm{p}_{\mathrm{rThigh}} = \mathrm{p}_{\mathrm{Hip}} + k\,(\mathrm{p}^{s}{}_{\mathrm{rThigh}} - \mathrm{p}^{s}{}_{\mathrm{Hip}}) \tag{12}$$

and

$$\mathrm{p}_{\mathrm{rThigh}} = \mathrm{p}_{\mathrm{Hip}} + k\,(\mathrm{p}^{s}{}_{\mathrm{rThigh}} - \mathrm{p}^{s}{}_{\mathrm{Hip}}) \tag{13}$$

where only the position $\mathrm{p}_{\mathrm{Hip}}$ is unknown, the k is the proportional coefficient and the superscript s denotes positions for the standard figure. Applying the rotation operator in Equations (12) and (13), and ignoring the rotation around x-axis, i. e., $\theta = 0$, we get

$$\mathbf{p}_{\mathrm{rThigh}} = \begin{pmatrix} x_{\mathrm{rThigh}} \\ y_{\mathrm{rThigh}} \\ z_{\mathrm{rThigh}} \end{pmatrix} = \begin{pmatrix} \cos\psi\cos\varphi & -\sin\varphi & \cos\psi\sin\varphi \\ \sin\psi\cos\varphi & \cos\psi & \sin\psi\sin\varphi \\ -\sin\varphi & 0 & \cos\varphi \end{pmatrix} \begin{pmatrix} l^0{}_{xr} \\ l^0{}_{yr} \\ l^0{}_{zr} \end{pmatrix} + \begin{pmatrix} x_0 \\ y_0 \\ z_0 \end{pmatrix} \tag{14}$$

and

$$\mathbf{p}_{\mathrm{lThigh}} = \begin{pmatrix} x_{\mathrm{lThigh}} \\ y_{\mathrm{lThigh}} \\ z_{\mathrm{lThigh}} \end{pmatrix} = \begin{pmatrix} \cos\psi\cos\varphi & -\sin\psi & \cos\psi\sin\varphi \\ \sin\psi\cos\varphi & \cos\psi & \sin\psi\sin\varphi \\ -\sin\varphi & 0 & \cos\varphi \end{pmatrix} \begin{pmatrix} l^0{}_{xl} \\ l^0{}_{yl} \\ l^0{}_{zl} \end{pmatrix} + \begin{pmatrix} x_0 \\ y_0 \\ z_0 \end{pmatrix} \tag{15}$$

with

$$\begin{pmatrix} l^0{}_{xl} \\ l^0{}_{yl} \\ l^0{}_{zl} \end{pmatrix} = \begin{pmatrix} x^0{}_{\mathrm{lThigh}} - x^0{}_{\mathrm{Hip}} \\ y^0{}_{\mathrm{lThigh}} - y^0{}_{\mathrm{Hip}} \\ z^0{}_{\mathrm{lThigh}} - z^0{}_{\mathrm{Hip}} \end{pmatrix}$$

and

$$\begin{pmatrix} l^0{}_{xr} \\ l^0{}_{yr} \\ l^0{}_{zr} \end{pmatrix} = \begin{pmatrix} -l^0{}_{xl} \\ l^0{}_{yl} \\ l^0{}_{zl} \end{pmatrix}.$$

From Equations (14) and (15), we finally obtain the rotation angles of hip segment,

$$\varphi = \sin^{-1}\left(-\frac{z_{\mathrm{lThigh}} - z_{\mathrm{rThigh}}}{l^0{}_{xl} - l^0{}_{xr}} \right) \tag{16}$$

and

$$\psi = \cos^{-1}\left[-\frac{x_{\mathrm{lThigh}} - x_{\mathrm{rThigh}}}{\left(l^0{}_{xl} - l^0{}_{xr}\right)\cos\varphi} \right]. \tag{17}$$

The unknown coordinates of the hip start point will then be calculated from Equation (14) or (15) with its rotation angles, Equations (16) and (17).

Results and Discussion

While there is a need to find anatomical landmarks at joints, infrared refractive markers are attached on the human body surface and measured with the motion analysis system. This indicates that the markers give no more than an approximate estimate of the joint center positions. Because of this, both the legs that became phantom-like intersected each other during the simulated treadmill walking. Therefore, the current program was revised to avoid the incorrect intersect but its problem remains opened.

We use a general algorithm for transforming coordinates of individual segments in a global frame of reference to those in its parent-fixed local frame of references. The Euler angle method gives us the 3 parent-fixed rotation angles that are needed as motion data in a BVH file, of the segments except the root. Thus, we should estimate unknown values of coordinates of the root from its neighboring coordinates, assuming the root is in geometric proportion to that of a standard figure given in Poser. This assumption is probably permitted since the treadmill walking is simulated well as shown in Figure 5.

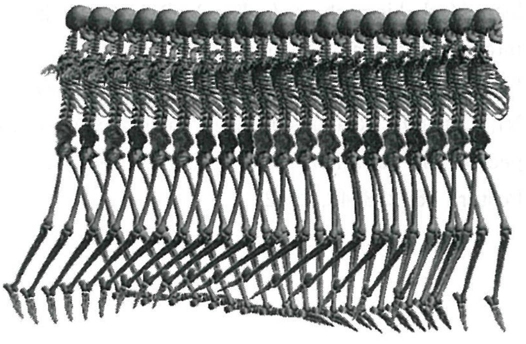

Figure 5. Simulated treadmill walking represented by a skeleton figure. The multiple Poser-image shows first 20 frames from totally 300 frames of the motion sequence of the walking person on a treadmill and its sequence was captured at a frame rate of 60 frames per second.

In the present study, we developed a Windows program, but not a Excel macro[7], that performs the following tasks: 1) it reads motion data as a CSV format file; 2) it converts positions of segments to rotation angles; and 3) it writes a BVH format file. The Windows program was examined by using a test CSV format file. Values of the variables were verified until the former 2 tasks were completed. For the latter task, the generated BVH format file was examined to be imported by Poser. It was concluded that the program itself works satisfactorily though the abnormal rotations remain open.

References

1) National Library of Medicine, 'The Visible Human Project®,' available from http://www.nlm.nih.gov/research/visible/visible_human.html; Internet; accessed 10 January 2003
2) Bry L, 'A Guided Tour of the Visible Human,' available from http://www.madsci.org/~lynn/VH/; Internet; accessed 10 January 2003
3) Flavin P, 'Bipedal Human Gait: A 3d Interactive Model with Animation,' available from http://www.frontiernet.net/~imaging/gait_model.html; Internet; accessed 10 January 2003
4) Schillings AM, Van Wezel BMH, Mulder Th, Duysens J, 'Stumbling over Obstacles during Human Treadmill

Walking in Young and Older Adults,' available from http://asb-biomech.org/onlineabs/NACOB98/292/; Internet; accessed 10 January 2003

5) Freber R, Ostering LR, Woollacott MH, Wasielewski NJ, Lee JH. Reactive balance adjustments to unexpected perturbations during human walking. Gait Posture 16: 238-48, 2002

6) BioVision, 'General BVH File Structure,' available from http://biovision.com/bvh.html; Internet; accessed 10 January 2003

7) Ohnishi A. Excel macro for animating DIFF data in Poser. Newsletter of the Clinical Gait Analysis Forum of Japan 35: 9, 2001